ICFO

**Institut
de Ciències
Fotòniques**

Ultrafast optical parametric oscillators

Novel systems, techniques, and concepts

Venkata Ramaiah-Badarla

Thesis Advisor
Majid Ebrahim-Zadeh
Thesis Co-Advisor
Adolfo Esteban-Martin

To my Family and Friends

Abstract

In this thesis, we have demonstrated various ultrafast optical parametric oscillators (OPOs) based on different nonlinear media. The thesis consists of OPO systems, novel techniques, designs, and concepts that has facilitated the wavelength accessibility from 1 μm in the *near-infrared* region to as far as 8 μm in the *mid-infrared* region.

We developed a *fs* OPO based on BiB_3O_6 (BIBO) directly pumped the Kerr-lens mode-locked (KLM) Ti:sapphire laser. This system could provide broad and rapid tuning from 1420-1560 nm just by changing the cavity length. Also, by exploiting the unique optical properties of BIBO under *type I* *(e→oo)* interaction, we have demonstrated the first self-phase-locked degenerate *fs* OPO. Further, we have developed a technique called synchronous retro-reflection for threshold reduction and signal amplification before the onset of the oscillation. This technique is generic and is particularly useful while deploying ultrafast OPOs with birefringent materials that have relatively low nonlinear gain and when we have limited pump power.

In addition, we have developed a dual-wavelength *fs* OPO with arbitrary and independent tuning by making use of anti-resonant-ring (ARR) or Sagnac interferometer. This universal technique of coupling two optical oscillators can be employed in any time regime (cw to ultrafast pico or *fs*) irrespective of the operating wavelengths. This conceptual technique can be used for intracavity terahertz (THz) generation which exploits the high intensity intracavity oscillating pulses. Also, we have developed a dual-crystal, double-pumped OPOs for intracavity signal amplification in *fs* regime as well as in ps regime, for arbitrary and independent wavelength tuning. In both systems two crystals share the same optical cavity but are pumped independently by a single laser source.

Finally, we have devised and experimentally demonstrated a novel concept of pumping an OPO within another OPO using a composite cascaded cavity design. This all solid-state Ti:sapphire-pumped *fs* OPO system is potentially capable of providing access to *mid-infrared* region beyond 4 μm to as far as 18 μm by careful selection of the nonlinear medium.

Resumen

En esta tesis, hemos demostrado varios osciladores ópticos paramétricos ultrarrápidos (OPO) basados en diferentes medios no lineales. La tesis consta de sistemas OPO, técnicas novedosas, diseños y conceptos que han facilitado el acceso a longitudes de onda de 1 μm en la región del infrarrojo cercano, así como hasta 8 μm en la región del infrarrojo medio.

Hemos desarrollado un femtosegundo (fs) OPO basado en BiB_3O_6 (BIBO) directamente bombeado por un láser Kerr-lens mode-locked (KLM) de Ti:zafiro. Este sistema proporciona amplia y rápida sintonización en el rango 1400-1560 nm con sólo cambiar la longitud de la cavidad. También, gracias a las propiedades ópticas únicas de BIBO en la interacción *tipo I (e→oo)*, hemos demostrado el primer fs OPO self-phaselocked degenerado. Además, hemos desarrollado una técnica llamada retro reflexión sincronizada para la reducción del umbral y amplificación de señal, antes de la aparición de la oscilación. Esta técnica es genérica y es particularmente útil para implementar OPOs ultrarrápidos con materiales birrefringentes que tienen relativamente baja ganancia no lineal y cuando existe una limitación de la potencia de bombeo. Adicionalmente, hemos desarrollado un fs OPO con longitud de onda dual que presenta sintonización arbitraria e independiente mediante el uso de un interferómetro de anillo antirresonante (ARR) o Sagnac. Esta técnica universal de acoplamiento de dos osciladores ópticos puede ser empleada en cualquier régimen temporal (desde *cw* a ultrarrápido de pico o femtosegundo) e independientemente de las longitudes de onda de operación. Esta técnica puede ser utilizada para la generación de THz intracavidad, permitiendo aprovechar la alta intensidad de los pulsos oscilantes.

Además, hemos desarrollado un sistema OPO de doble cristal y doble bombeo para la amplificación de la señal dentro de la cavidad tanto en régimen de fs como de ps, para el ajuste de longitud de onda arbitraria e independiente. En ambos sistemas los dos cristales comparten la misma cavidad óptica, pero son bombeados independientemente por una sola fuente láser.

Por último, hemos diseñado y demostrado experimentalmente un concepto novedoso para bombear un OPO dentro de otro OPO mediante un diseño de

cavidad compuesta en cascada. Este sistema de estado sólido OPO de femtosegundo bombeado por el láser de Ti: zafiro es potencialmente capaz de proporcionar acceso a la región del infrarrojo medio más allá de 4 μm incluso hasta las 18 μm, realizando una cuidadosa selección del medio no lineal.

Acknowledgements

First of all, I would like to express my sincere gratitude to Prof. Majid Ebrahim-Zadeh, for giving me the opportunity to conduct research in his group. Also, I thank Dr. Adolfo Esteban-Martin my co-advisor, for rendering his continuous support in the lab during the last four years. The various discussions among the group have been very fruitful and inculcated in me intellectual skills such as critical thinking, consistency, research design and problem-solving. I acknowledge the kind and helping nature of my colleagues in the group - Gautam, Chaitanya, Kavita, Enrique and Ossi. I really appreciate your help in various aspects that made my working environment enjoyable and happier. I would also like to thank the different units at ICFO such as administration, KTT, mechanical, electronic, IT and logistics for their help and organised coordination.

I am indebted to my parents, sister (Indira) and brother (Manoj) for their unconditional love, affection and encouragement. I would also like to thank Rev. Jacob John and Charles John whose teachings have/had made a profound impact in my life. ICFO has been a marvellous institution not only for research but also a place with various seasonal activities which keeps you always refreshed. Here I got the opportunity to meet many wonderful people from different countries and continents. Thanks to all of my friends at ICFO who made my times in and outside ICFO memorable. I thank Yannick, Anaid, Isabel, Claudia, Valeria, Mariale, Kenny, Camila, Jiri, Luis and Alberto for inviting me to various fiestas. The late night discussions with Alberto Curto and his hard-working nature has always motivated me. I would also like to thank Mathieu Mivelle, Kyra, Gaetan for various suggestions, barbecues and hangouts. I would like to specially thank my best pals at ICFO Roberto (LB), Rafa (Greyiish), and Alex (Zamora) with whom I always felt and will feel cherished. Anshuman, you have been my second mentor, philosopher friend and a dear well wisher, many thanks for listening to me at hard times and for all those prudent suggestions. I also thank the Indian community (Dhriti, Arup, Saurabh, Hari Varma, Amit (Thursday), Venkatesh, Kavita jr.) at ICFO for those food festivals, get together and din-

Journal publications

1. **V. Ramaiah-Badarla**, A. Esteban-Martin, S. Chaitanya Kumar, K. T. Zawilski, P. G. Schunemann, and M. Ebrahim-Zadeh, "Ti:sapphire-pumped, deep-mid-infrared optical parametric oscillator based on $CdSiP_2$ tunable across 6-8 μm," (submitted)

2. **V. Ramaiah-Badarla**, A. Esteban-Martin and M. Ebrahim-Zadeh,"Double-crystal, dual-synchronously-pumped femtosecond optical parametric oscillator," (submitted)

3. **V. Ramaiah-Badarla**, S. Chaitanya Kumar, and M. Ebrahim-Zadeh,"Fiber-laser-pumped, dual-wavelength, picosecond optical parametric oscillator," Opt. Lett. **39**, 2739-2742 (2014).

4. **V. Ramaiah-Badarla**, A. Esteban-Martin, and M. Ebrahim-Zadeh, "Self-phase-locked degenerate femtosecond optical parametric oscillator based on BiB_3O_6," Laser Photonics Rev. **7**, L55-L60 (2013).

5. A. Esteban-Martin, **V. Ramaiah-Badarla**, and M. Ebrahim-Zadeh, "Dual-wavelength optical parametric oscillator using antiresonant ring interferometer," Laser Photonics Rev. **6**, L7-L11 (2012).

6. A. Esteban-Martin, **V. Ramaiah-Badarla**, and M. Ebrahim-Zadeh, "Synchronized retro-reflection-pumped femtosecond optical parametric oscillator," Opt. Lett. **37**, 1091-1093 (2012).

7. A. Esteban-Martin, **V. Ramaiah-Badarla**, V. Petrov, and M. Ebrahim-Zadeh, "Broadband, rapidly tunable Ti:sapphire-pumped bismuth triborate femtosecond optical parametric oscillator," Opt. Lett. **36**, 1671-1673 (2011)

Conference papers

1. **V. Ramaiah-Badarla**, A. Esteban-Martin, S. Chaitanya Kumar, K. Devi, K. Zawilski, P. Schunemann, M. Ebrahim-Zadeh," Ti:sapphire-pumped, deep-mid-infrared, intracavity-cascaded femtosecond optical parametric oscillator," Euro Photonics Conference, Nauchatel, Switzerland, August, 2014.

2. **V. Ramaiah-Badarla**, A. Esteban-Martin, S. Chaitanya Kumar, K. Devi, K. Zawilski, P. Schunemann, M. Ebrahim-Zadeh," $CdSiP_2$ optical parametric oscillator tunable across 6-8 μm synchronously pumped by a Ti:sapphire laser," Advanced Photonics Congress, Barcelona, July, 2014.

3. **V. Ramaiah-Badarla**, S. Chaitanya Kumar, and M. Ebrahim-Zadeh,"Yb-Fiber-Laser-Pumped, High-Power, High-repetition-rate Dual-Wavelength Picosecond Optical Parametric Oscillator," Conf. Lasers and Electro-Optics (CLEO), San Jose, California, USA, May 2014.

4. **V. Ramaiah-Badarla**, A. Esteban-Martin, and M. Ebrahim-Zadeh, "Self-phase-locked sub-harmonic femtosecond optical parametric oscillator based on BiB_3O_6," Frontiers in optics, Orlando , Florida, USA , October 2013

5. A. Esteban-Martin, **V. Ramaiah-Badarla**, and M. Ebrahim-Zadeh," Dual-wavelength synchronously-pumped femtosecond optical parametric oscillator using antiresonant ring interferometer," CLEO/Europe-EQEC, Munich, Germany, May 2013

6. **V. Ramaiah-Badarla**, K. Devi, S. Chaitanya Kumar, A. Esteban-Martin, M. Ebrahim-Zadeh, "Interferometrically coupled two-color femtosecond optical parametric oscillator," The International Conference on Fiber Optics and Photonics, Madras, India, December 2012.

7. **V. Ramaiah-Badarla**, A. Esteban-Martin, and M. Ebrahim-Zadeh, "Interferometrically-coupled, dual-wavelength femtosecond optical parametric oscillator," NLO 50 International Symposium, Barcelona, Spain, October 2012 .

8. A. Esteban-Martin, **V. Ramaiah-Badarla**, and M. Ebrahim-Zadeh, "Synchronized retro-reflection-pumped femtosecond optical parametric oscillator," CLEO, San Jose, USA, May 2012.

9. A. Esteban-Martin, **V. Ramaiah-Badarla**, V. Petrov, and M. Ebrahim-Zadeh, "Broadband, rapidly tunable, BiB_3O_6 femtosecond optical parametric oscillator directly pumped by a Ti:sapphire," CLEO/ Europe-EQEC 2011, Munich, Germany, May 2011.

Patents

M. Ebrahim-Zadeh, **V. Ramaiah-Badarla**, A. Esteban-Martin, S. Chaitanya Kumar "Internally cascaded optical parametric oscillators" (International patent).

Contents

Chapter 1

Introduction

1.1 Background

Nonlinear optics is the study of optical manifestations of the dielectric medium when subjected to *intense optical electromagnetic fields*. Though several nonlinear optical phenomena such as *Kerr*, *Pockel*, and *Raman* effects were known till early twentieth century, the true visibility for nonlinear optical frequency conversion processes was enabled only after the invention of the light amplification by stimulated emission of radiation (LASER) [1] in 1960. This was rapidly followed by the milestone experiment of optical harmonics generation by Franken [2] in 1961 popularly known as second harmonic generation (SHG). Soon afterwards, sum frequency generation (SFG) was reported by Bass [3]. Both of these experiments suffered from the effects of dispersion due to different phase velocities of the interacting waves inside the non-centrosymmetric nonlinear media (quartz and tri glycine sulphate crystals), thus resulting in poor conversion efficiency. In 1962, Giordmaine [4] and Maker [5] independently put forward the idea of phase-matching and described how birefringent materials can be used to offset the phase-mismatch (or also known as conservation of *electromagnetic* momentum). The exploitation of birefringence to phase-match the interacting fields in a non-centrosymmetric medium is popularly known as birefringent phase-matching. Another means of phase-matching was suggested by

Armstrong [6] called quasi-phase-matching (QPM) which involves periodic modulation of the sign of the nonlinear coefficient of the medium to compensate for the phase-mismatch. Later the experiments of sum frequency generation (SFG) [7] and optical rectification (OR) [3] were demonstrated in potassium dihydrogen phosphate (KDP), ammonium dihydrogen phosphate (ADP) and potassium di deuturium phosphate (KD*P) respectively. In 1965, the first *near-infrared* tunable nanosecond (ns) optical parametric oscillator (OPO) based on lithium niobate ($LiNbO_3$) was reported by Giordmaine [8], followed by difference frequency generation (DFG) into *far-infrared* in Quartz by Zernike [9]. Later in 1968, Byer [10] reported the first continuous-wave (*cw*) *visible* OPO based on $LiNbO_3$.

As one can see, in less than eight years after the invention of laser, all the second order nonlinear parametric processes and devices such as SHG, SFG, OR, DFG and OPOs were demonstrated to conquer the various regions of the *electromagnetic* spectra not accessible through lasers. *This proves the strength of all second order nonlinear optical devices - Tunability.*

With the development of laser technology in conjunction with the discoveries of new and novel nonlinear media, unprecedented progress has been achieved in the field of nonlinear optics. During the past fifty years several optical parametric sources have been developed in various spectral and temporal regimes. Among these devices, especially, OPOs have now established themselves as viable and reliable sources for coherent generation of radiation by bridging various gaps in the *electromagnetic* spectrum all the way from *ultraviolet* (*UV*), *visible*, *near-infrared* to as far as *mid-infrared* regions [11]. The OPOs can be classified into three broad categories depending on the temporal regimes - continuous-wave (*cw*), nanosecond (*ns*), ultrafast picosecond (*ps*) and femtosecond (*fs*). In the context of this thesis, we focus mainly on ultrafast optical parametric oscillators, also known as synchronously-pumped optical parametric oscillators (SPOPOs). The first report of a *fs* SPOPO was made by Edelstein [12] in 1989, based on potassium titanyl phosphate ($KTiOPO_4$ or KTP) as a nonlinear medium and pumped by a colliding pulse-mode-locked dye laser. To access the high intensities necessary to reach the oscillation threshold, the KTP crystal was

deployed at the intracavity focus of the dye laser and the SPOPO produced milliwatts of average power under singly-resonant operation mode. In a similar SPOPO,with external pumping, Mak [13] reported generation of nearly 30 mW of average power.

However, the progress in fs SPOPO technology was triggered with the invention of Kerr-lens-mode-locked (KLM) Ti:sapphire [14] laser by Spence [15] in 1990. In 1992, Fu [16] and Pelouch [17] independently reported two different SPOPOs based on KTP pumped by high repetition rate (76 MHz) KLM fs Ti:sapphire laser. Since then, the KLM fs Ti:sapphire laser has been adopted as the workhorse for pumping SPOPOs in fs regime. In the following years, using the KLM fs Ti:sapphire laser as the pump source, several SPOPOs were reported based on various nonlinear media such as KTP [18], KTA ($KTiOAsO_4$) [19], [20], CTA ($CsTiOAsO_4$) [21], [22], RTA ($RbTiOAsO_4$) [23], [24], LBO (LiB_3O_5) [25] for accessing the spectral regions from $near$-to-mid-$infrared$ (1-5 μm) under critical and non-critical phase-matching conditions. The spectral range of KLM Ti:sapphire-pumped fs SPOPOs has also been extended into $visible$ region either by intracavity SHG of the SPOPO signal pulses [26], [27] or through intracavity SFG between the pump and oscillating signal pulses [28] in a suitable nonlinear media like β-barium borate, (β-BaB_2O_4 or BBO). Both approaches exploited the high intracavity oscillating signal intensities inside the SPOPOs. A $visible$ fs SPOPO was reported by Driscoll [29] in 1994 based on BBO as the nonlinear medium pumped by the second harmonic of the KLM Ti:sapphire laser at $\sim$400 nm.

The early 1990's can be considered as a culmination of two important technologies that paved the way for development of ultrafast fs SPOPOs. One being the invention of KLM Ti:sapphire in the laser technology and the other being the matured crystal growth technology for periodically poling the ferroelectric materials like $LiNbO_3$. While the KLM fs Ti:sapphire established itself as reliable and robust all-solid-state laser, the periodic poling [30], [31] enabled the possibility of bringing QPM into action, nearly three decades after the first postulation in 1962 [6]. In 1997, there were two independent demonstrations of Ti:sapphire-pumped SPOPOs based on periodically poled

lithium niobate (PPLN), and periodically poled RTA (PPRTA) by Burr [32] and Reid [33], respectively. This was followed by several SPOPOs based on PPKTP and its isomorphs [34], [35], [36].

Later in 2006, a *fs* SPOPO was reported by our group [37] based on bismuth triborate (BiB_3O_6) as nonlinear medium. However, this SPOPO was pumped by second harmonic of the Ti:sapphire laser at ~ 400 nm and provided a gap-free tuning all the way from 350 nm in the UV to 2500 nm in the *near-infrared* region. After this, a *fs* SPOPO directly pumped by KLM Ti:sapphire was reported by Kalyan [38] based on periodically poled stoichiometric lithium tantalate ($PPSLT$). Quite recently, in 2011 we demonstrated a *fs* SPOPO directly pumped by a Ti:sapphire laser based on BiB_3O_6 [39]. Thus, one can clearly see the progress achieved in the ultrafast *fs* SPOPOs based on various nonlinear media by using solid-state KLM Ti:sapphire *fs* laser as the pump source over the last 23 years.

1.2   Overview

This thesis presents various ultrafast SPOPOs based on different nonlinear crystals. This includes systems, designs, techniques and novel concepts that have enabled access to spectral regions from 1 μm in the *near-infrared* to as far as 8 μm in the deep mid-infrared (MIR) region. Throughout this thesis, the KLM Ti:sapphire was used as the pump source for developing various *fs* SPOPOs except in one chapter where we have used a picosecond Yb-fiber laser.

The thesis has been organised as follows:

Chapter 2 includes the basic theory of nonlinear optics with a focus on second-order nonlinear optical processes such as SHG, SFG, DFG, OPG and OPOs. Also, some important phenomena like group velocity, group velocity mismatch, group velocity dispersion and compensation are described, which are vital in the *fs* regime.

In chapter 3, we describe a *fs* SPOPO based on BiB_3O_6. This system can be rapidly tuned from 1420 to 1580 *nm* in the *near-infrared* region just by changing the cavity length of the OPO. Though several SPOPOs have been developed previously in our group based on BiB_3O_6, this is the first demonstration of such a *fs* SPOPO based on BiB_3O_6 directly pumped by KLM Ti:sapphire laser.

In chapter 4, we describe a technique of synchronous retro-reflection of the pump. This technique involves retro-reflection of the undepleted pump back into the SPOPO cavity for signal amplification and pump threshold reduction even before the onset of the oscillation. This technique is particularly important for the ultrafast SPOPOs while deploying the birefringent nonlinear media with relatively low nonlinear coefficients and limited available pump powers.

In chapter 5, we demonstrate the first self-phase-locked degenerate *fs* SPOPO based on a birefringent nonlinear crystal - BiB_3O_6. By exploiting the inherent and unique optical properties of BiB_3O_6 under *type I(e→oo)* phase-matching, we have generated a stable degenerate output spectrum of 46 *nm*, when pumped with a 7 *nm* bandwidth Ti:sapphire laser pulses centred at 800 *nm*. The true phase-locking mechanism was verified using *f*-2*f* interferometer along with the RF measurements.

In chapter 6, we describe a novel and universal technique to couple two SPOPO cavities using Anti Resonant Ring (ARR) or Sagnac interferometer. Using this technique, we have coupled two separate *fs* SPOPOs that can provide independent and arbitrarily tunable wavelengths without any coherent coupling between the two nonlinear media. The technique has a potential impact especially in the context of terahertz (THz) generation through difference frequency mixing inside an optical cavity by exploiting the high intra-cavity intensities of the two independently oscillating fields inside the ARR. This technique can be employed in any time domain from *cw* to ultrafast *fs*, irrespective of the operating wavelengths.

In chapter 7, we have designed and demonstrated a double-crystal, dual-synchronously-pumped SPOPO system in picosecond regime that has facilitated independent and arbitrary tuning of wavelengths. This system could provide Watt level signal output and can be used to generate THz radiation external to the cavity by doing DFG in a suitable nonlinear medium like DAST or ZnTe.

In chapter 8, we present a dual-crystal, dual-synchronously-pumped *fs* SPOPO for intracavity signal amplification based on MgO:PPLN as a nonlinear medium. Two MgO:PPLN crystals are deployed in a single cavity and are pumped synchronously with a common pump source. This scheme shows how the interaction length can be increased without compromise on the gain bandwidth.

Finally, in chapter 9, we have devised and developed a new, simple, novel and universal concept of developing an OPO within another OPO. This novel concept and design has the potential to develop all-solid-state-pumped tunable OPOs that can provide wavelength tunability from 1 *μm* in the *near-infrared* to as far as 18 *μm* in the *mid-infrared* region depending upon the careful selection of the nonlinear media.

Chapter 10 consists the overall summary and an outlook of the presented work.

Chapter 2

Basic principles of nonlinear optics

2.1 Introduction to nonlinear optics

The description of nonlinear optical effects is based on the extension of the motion of linear propagation of the *electromagnetic fields* in a dielectric medium. It relies on the use of Maxwell's equations in which the polarisation of the medium is expressed by means of a power series expansion of the amplitude field present in the medium. In the same manner as the linear properties of the medium are described by the quantity called *susceptibility*, the nonlinear properties are characterised by certain number of nonlinear susceptibilities. To modify the properties of material, it is necessary to use a coherent light source like laser that is sufficiently intense. The first observation of nonlinear optical effects dates back to 1961, when Franken demonstrated optical second harmonic generation in a quartz crystal. Previously it was thought that linear properties of a medium are described by means of one complex quantity only - *The susceptibility.* The induced polarisation of a medium in presence of applied electric field is defined as

$$P = \epsilon_o \chi^{(1)} E \tag{2.1}$$

where $\chi^{(1)}$ is the linear susceptibility of the medium and this relation shows the linear dependence of polarisation (dipole moment per unit volume) on the strength of the applied *electromagnetic field*. When the applied electric field is intense enough, the induced polarisation is no longer linear and the non-linear properties of the medium are characterised by higher order nonlinear susceptibilities. Thus, the polarisation term can be expressed as

$$P = \epsilon_o[\chi^{(1)}E + \chi^{(2)}E.E + \chi^{(3)}E.E.E + ...] \qquad (2.2)$$

where $\chi^{(2)}$, $\chi^{(3)}$ are the second- and third-order nonlinear optical susceptibilities. As a consequence of the nonlinear dependence of the polarisation, the orientation of the induced polarisation differs from that of the applied optical electric field. Also, for an anisotropic medium to exhibit the second-order nonlinearity, the material must be non-centrosymmetric as proved below. In case of centrosymmetric medium, the inversion symmetric operation is defined as

$$I_{op}(F) = -F \qquad (2.3)$$

where F is a material property and from equation 2.2, one can write that

$$-P = \epsilon_o[-\chi^{(1)}E - \chi^{(2)}E.E - \chi^{(3)}E.E.E + ...] \qquad (2.4)$$

If the medium is centrosymmetric, then the following relations are applicable:

$$I_{op}(P) = -P \qquad (2.5)$$

and

$$I_{op}(E) = -E \qquad (2.6)$$

Applying the symmetry operation on 2.2 gives

$$I_{op}(P) = -P = \epsilon_o[-\chi^{(1)}E + \chi^{(2)}E.E - \chi^{(3)}E.E.E + ...] \qquad (2.7)$$

By comparing 2.4 and 2.7, consistency exits only if

$$\chi^{(2)}E.E = -\chi^{(2)}E.E \qquad (2.8)$$

Hence, $\chi^{(2)}$ must be zero and any media with inversion symmetry has $\chi^{(2n)}$ = 0. Thus, to exhibit a second order non-linearity, the medium must be non-centrosymmetric.

In this thesis, we restrict ourselves to various optical processes related to second-order nonlinear susceptibility. More commonly, the susceptibility is represented by the so-called d-coefficients given by $\chi_{ijk}^{(2)} = 2d_{ijk}$. The susceptibility ($\chi_{ijk}$) and the nonlinear coefficient (d_{ijk}) are tensors of rank 3 containing 3^{n+1} elements with n being the order of susceptibility. The index i can have values 1, 2, 3 corresponding to the respective crystal axes x, y, z, and jk can have values 1, 2, 3, 4, 5, 6 corresponding to the combinations of axes $xx, xy=yx, yy, yz=zy, zx=xz, and zz$. In practice, the d-coefficients are used to analyse the nonlinear interactions by using the d-matrix depending on the crystallographic point group. Also, the effective nonlinear coefficient (d_{eff}) depends on the direction of propagation of light within the crystal, polarisation direction, and the orientation of the crystal as well.

2.2 Optical parametric processes and devices

If we consider an optical field consisting of two distinct frequency components, ω_1 and ω_2, incident upon the nonlinear medium, which can be represented by

$$E(t) = E_1(t)\exp(-i\omega_1 t) + E_2(t)\exp(-i\omega_2 t) + c.c \qquad (2.9)$$

Then, the second-order nonlinear polarisation can be expressed as

$$P^{NL} = \chi^{(2)}E^2(t) \qquad (2.10)$$

Substituting equation 2.9 in 2.10, we get

$$P^{NL} = \epsilon_o\chi^{(2)}[E_1^2(t)\exp(-2i\omega_1 t) + E_2^2(t)\exp(-2i\omega_2 t) + 2E_1E_2\exp(-i(\omega_1+\omega_2)t$$
$$+ 2E_1E_2^*\exp(-i(\omega_1-\omega_2)t + c.c.] + 2\epsilon_o\chi^{(2)}[E_1E_1^* + E_2E_2^*] \quad (2.11)$$

Thus, from the above equation, we can conclude that an optical parametric process of three-wave interaction consists of the following frequency mixing processes. The first two terms describe the SHG processes, the third term describes the SFG, while the fourth term describes the DFG, and the last term describes the OR process. SHG can be considered as a special case of SFG in which $\omega_1 = \omega_2$. The various second-order nonlinear optical processes are depicted in the *Fig.* 2.1.
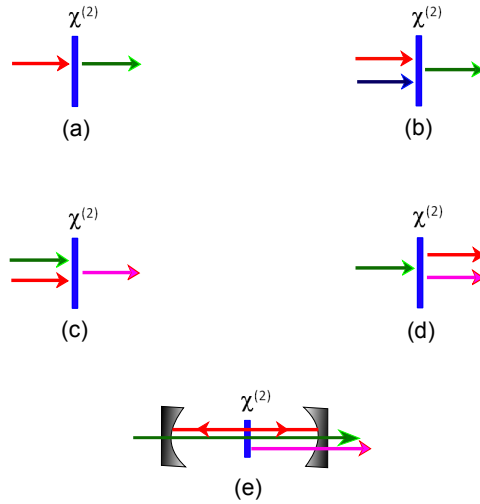
Figure 2.1: Various second-order nonlinear optical processes in a non-centrosymmetric medium (a) SHG (b) SFG (c) DFG (d) OPG (e) OPO.

Optical parametric generation (OPG) is a process in which an input pump photon at high frequency ω_p is split into two photons of lower frequencies in the nonlinear medium. The field at ω_p generally corresponds to an intense input optical field called *pump*, giving rise to a pair of generated fields at frequencies ω_s and ω_i. The generated field at the higher frequency is referred

to as *signal*, while the field at lower frequency is termed as *idler*. This process is also known as *parametric down-conversion*. In all the three wave interaction processes, both conservation laws - energy and momentum (or phase-matching) must be satisfied such that

$$\omega_p = \omega_s + \omega_i \tag{2.12}$$

$$\Delta k = k_p - k_s - k_i = 0 \quad \text{or} \quad n_p\omega_p - n_s\omega_s - n_i\omega_i = 0 \tag{2.13}$$

where $n_{p,s,i}$ are the respective refractive indices of *pump, signal* and *idler*. The generated *signal* and *idler* wavelengths are governed by the above two conservation conditions. The down-conversion process generates a very weak *signal* called *parametric fluorescence*. To obtain appreciable amount of conversion efficiency, either we need a very strong pump intensity or the nonlinear medium should posses very high nonlinear coefficient under proper phase-matching conditions. Thus, to increase the conversion efficiency, two parametric sources or devices are generally used for practical applications.

One being the *optical parametric amplifier* (OPA), the other is called *optical parametric oscillator* (OPO). OPAs are pumped by high-power lasers like regenerative amplifiers which possesses very large peak intensity (GW/cm^2) and hence *parametric super-fluorescence* can be generated in a single pass configuration. However, OPAs consists of multiple stages through which the generated parametric fluorescence is amplified in successive stages with a proper delay between the generated *signal* and the *pump* pulses inside the nonlinear crystal. On the other hand, if we deploy the nonlinear crystal inside an optical resonator that could provide feedback for amplification, such a device is known as *optical parametric oscillator* (OPO). The major difference between an OPA and OPO can be described as follows:

An OPA requires extremely powerful (*mJ*) pump pulses in *ps* or *fs* duration and operate in a single pass configuration with very low repetition rate typically at 1 *KHz*. On the other hand, OPOs can be operated at much low pump energy (*nJ* pulses) and at high repetition rates (76 to 100 *MHz*).

Also, one has to note the major difference between a laser and an OPO. While both laser and OPO consist of optical cavities, the gain in an OPO is

instantaneous unlike in the laser where the emission is governed by population inversion. *Thus, in OPOs there is no storage of energy.* In a laser, the tunability depends on the bandwidth of the electronic transitions whereas in OPOs the tunability is achieved by phase-matching conditions in conjunction with the energy conservation laws. Especially in the ultrafast *fs* regime, since gain is instantaneous, it is necessary to use the scheme of *synchronous pumping* in which the cavity length of the OPO needs to be matched exactly with the repetition rate of the pump laser.

2.3 Coupled wave equations

The coupled wave equations are the important tools to investigate the various optical parametric processes involving any three-wave interactions like - SHG, SFG and DFG in a nonlinear medium. For a lossless, non-conducting, and non-magnetic medium, the coupled equations with *slowly varying envelope approximation (SVEA)* can be written as follows:

$$\frac{\partial}{\partial z}E_1(z) = \frac{2id_{eff}\omega_1^2}{k_1c^2}A_3A_2^*exp(i\Delta kz) \tag{2.14}$$

$$\frac{\partial}{\partial z}E_2(z) = \frac{2id_{eff}\omega_2^2}{k_2c^2}A_3A_1^*exp(i\Delta kz) \tag{2.15}$$

$$\frac{\partial}{\partial z}E_3(z) = \frac{2id_{eff}\omega_3^2}{k_3c^2}A_1A_2exp(-i\Delta kz) \tag{2.16}$$

where E_i(z) are the amplitudes of the electric fields of interacting waves, d_{eff} is the effective nonlinear coefficient, and $\Delta k = k_3$ - k_2 - k_1 is the momentum or wave vector mismatch between the interacting fields.

The three basic equations imply that the amplitude of the newly produced wave is coupled to the incoming waves through the nonlinear coefficient (d_{eff}) [40], [41]. There is energy flow from waves at frequencies ω_1 and ω_2 to the wave at frequency ω_3. At the same time, inverse process can also take place, i.e.,

the process in which the newly generated frequency ω_3 mixes with one of the two incoming waves called difference frequency mixing ($\omega_1 = \omega_3 - \omega_2$).

2.4 Phase-matching

Phase-matching or conservation of *electromagnetic* momentum was proposed separately by Giordmaine [4] and Maker [5] in 1962. *It is a technique in which the phase velocity mismatch between the interacting waves could be offset by exploiting the inherent characteristics of an anisotropic nonlinear medium.* In a three-wave interaction process, physically it represents that the value of Δk should somehow be made equal to zero ($k_1 - k_2 - k_3 = 0$). Phase-matching can be realized by different methods which will take the advantage of the fact that the refractive index changes as a function of incident angle, temperature and wavelength. The case in which $\Delta k = 0$ is known as perfect phase-matching.
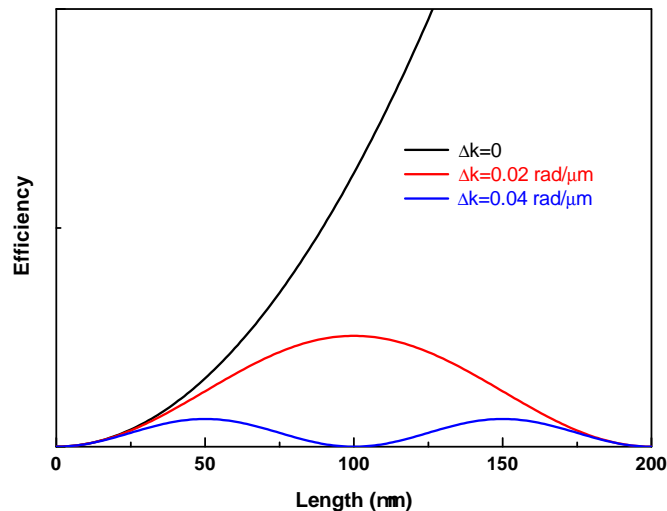
Figure 2.2: Dependence of efficiency on phase-mismatch between the interacting waves along the crystal length for SHG process.

However, in general, due to dispersion, optical waves at different frequencies travel with different phase velocities as they propagate through the nonlinear medium. Thus, after travelling a short distance known as the coherence length ($l_c = \frac{\pi}{\Delta k}$), the relative phase of the interacting waves slips by 180°. So, along the propagation direction inside the nonlinear medium, the

waves step in and out of phase periodically, resulting in exchange of energy back and forth. This periodic oscillation along the propagation length is shown in $Fig.$ 2.2. To offset the phase-mismatch, two techniques are widely used in nonlinear optics:

1. Birefringent phase-matching (BPM)
2. Quasi-phase-matching (QPM)

2.4.1 Birefringent phase-matching (BPM)

This is the most commonly known and widespread technique for achieving phase-matching in which the birefringence of a nonlinear crystal is exploited to offset the phase-velocity-mismatch. Birefringence is the property of anisotropic optical materials, where the refractive index of the material depends on the polarisation and propagation direction of light. When the interacting waves at different frequencies are polarised differently, their corresponding phase velocities can be adjusted, such that the index difference due to dispersion is balanced through the birefringence. In anisotropic materials, there exists normal modes of propagation for each frequency. These waves are orthogonally polarised and travel with different phase velocities. One of these waves, called $ordinary$ wave, experiences a constant index of refraction independent of the direction of propagation known as $ordinary$ index (n_o). The second wave, experiences different refractive index depending upon the direction of propagation, hence is called as $extraordinary$ index (n_e). The angle θ describes the direction of propagation relative to one of the principal axes of the medium. Depending upon the number of optical axes, a birefringent crystal can be divided into two categories, $uniaxial$ (single optical axis) and $biaxial$ crystals (two optical axes). With θ being the angle between wave-vector and the optic axis, the refractive index of $extraordinary$ wave is given by

$$\frac{1}{n_e^2(\theta)} = \frac{cos^2\theta}{n_o^2} + \frac{sin^2\theta}{\bar{n_e}^2} \tag{2.17}$$

28

From the above equation, one can deduce the following:

$$at \ \ \theta = 0° \ \ ; \ \ n_e(0) = n_o \tag{2.18}$$

$$at \ \ \theta = 90° \ ; \ \ n_e(90) = \bar{n}_e \tag{2.19}$$

Depending upon the polarisation of the interacting waves, the BPM can be classified into two types known as *type I* and *type II*. For OPO - *type I* phase-matching refers to the situation where the *signal* and *idler* have the same polarisations, whereas in *type II* phase-matching, the *signal* and *idler* have orthogonal polarisations. For SHG process - in *type I* phase-matching, the *pump* wave has either *ordinary* or *extraordinary* polarisation, while the generated SHG field is orthogonal to the input *pump* field *(ee→o or oo→e)*. In *type II* phase-matching, the *pump* is polarised in such a way that one of its orthogonal components is *ordinary* and the other is *extraordinary (eo→e or oe→o)*.

The birefringence Δn is defined as $n_e - n_o$. Depending upon the magnitude of this Δn, anisotropic crystals are divided into *positive* $(\Delta n > 0)$ and *negative* $(\Delta n < 0)$ uniaxial crystals, as shown in the *Fig.* 2.3.
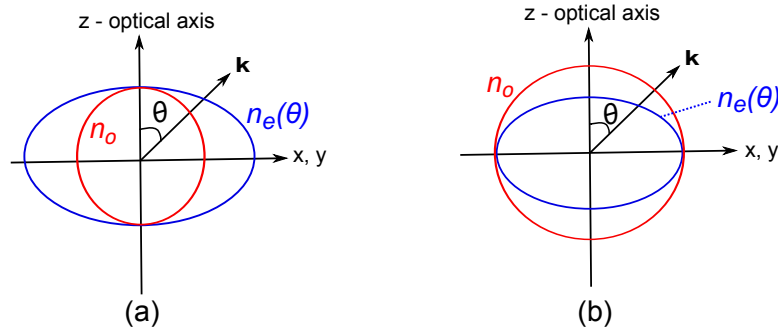

Figure 2.3: Index ellipsoid for (a) positive and (b) negative uniaxial crystal.

Also depending upon the angle θ with respect to the optical axis, the phase-matching is categorised into two types.

1. Non-critical phase-matching (NCPM)
2. Critical phase-matching (CPM).

If $\theta = 90°$, it is called non-critical phase-matching (NCPM), otherwise it is known as critical phase-matching (CPM). Whenever the angle θ between the propagation direction and the optical axis has a value other than 90°, the Poynting vector **S** and the propagation vector **k** are not parallel for *extraordinary* rays. As a result, *ordinary* and *extraordinary* rays with parallel propagation vectors quickly diverge from one another as they propagate through the crystal. This phenomenon is known as *spatial walk-off (or) Poynting vector walk-off*. This effect limits the spatial overlap of the two interacting waves and decreases the efficiency of any nonlinear frequency conversion process. The walk-off angle (ρ) is given by

$$\tan \rho = \frac{-1}{n_e} \frac{dn_e}{d\theta} \tag{2.20}$$

Thus, after a distance, denoted as the walk-off distance, the interacting beams will be completely separated from each other, causing a reduction in the intensity of the generated beam. Further, if the crystal length is much longer than the walk-off distance or aperture length (l_a), walk-off will severely hamper the growth of the generated beams. The relation between the walk-off angle ρ and aperture length l_a is given by

$$l_a = \frac{\sqrt{\pi}\omega}{\rho} \tag{2.21}$$

where ω is the radius of the Gaussian beam spot of *signal* or *idler* in an OPO.

The difference between the non-critical and critical phase-matching is depicted in the *Fig.* 2.4. In the case of critical phase-matching, a small deviation from perfect phase-matching will reduce the conversion efficiency considerably. While in the case of non-critical phase-matching, a small angle mismatch (induced by small angle tuning of the crystal) will only have minor effect on the conversion efficiency.
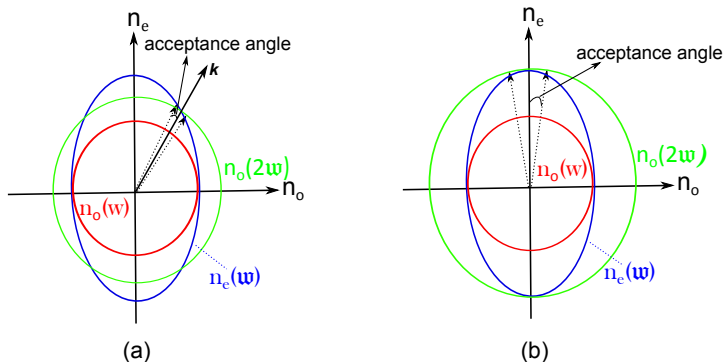
Figure 2.4: Phase-matching in a uniaxial birefringent crystal for a SHG process showing the distinction between (a) critical and (b) non-critical phase-matching.

The acceptance angle $\delta\theta$ is defined as follows: If the phase-matching angle θ_{PM} is tuned to $\theta_{PM} + \delta\theta$, the intensity of the generated field shall drop to half of its peak intensity, i.e., the acceptance angle gives the deviation from the phase-matching angle θ_{PM} for which the generated field intensity decays to half of its peak value. This deviation is characterized by the quantity $\Delta k L/2$ for which the function $\text{sinc}^2(\Delta k L/2) = 0.5$ for $\theta = \theta_{PM} + \delta\theta$ with L being the crystal length.

Thus NCPM is always advantageous over critical PM for two reasons. First, it is less sensitive to the acceptance angle and second, the walk-off angle is zero, which reduces the constraint on beam size and the effective crystal length.

In biaxial crystals, there exists two optical axes, which by convention are taken to lie in the optical xz plane. The optical axes are situated symmetrically about the z-axis as shown in $Fig.$ 2.5. The optical axes makes an angle of Ω with respect to the z-axis, given by

$$\sin\Omega = \frac{n_z}{n_y}\sqrt{\frac{n_y^2 - n_x^2}{n_z^2 - n_x^2}} \tag{2.22}$$
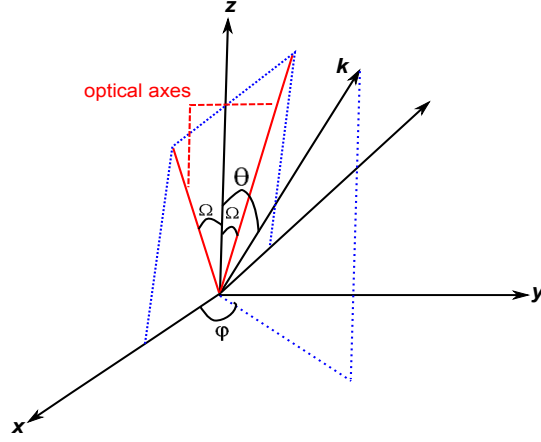
31

Figure 2.5: Crystallographic coordinate system for a biaxial crystal.

By convention, it is taken as $n_z > n_y > n_x$ and for the light propagating along the optical axes, the refractive index is independent of polarisation. The refractive indices of the two allowed modes of propagation are determined by solving the Fresnel's equation given by:

$$\frac{sin^2\theta cos^2\phi}{n^{-2} - n_x^{-2}} + \frac{sin^2\theta sin^2\phi}{n^{-2} - n_y^{-2}} + \frac{cos^2\theta}{n^{-2} - n_z^{-2}} = 0 \qquad (2.23)$$

where θ is the angle with respect to the z-axis and ϕ is the azimuthal angle with respect to x-axis. More detailed description about the phase-matching for various nonlinear frequency processes in biaxial crystals can be found in [42].

2.4.2 Quasi-phase-matching (QPM)

Quasi-phase-matching is an alternative technique to birefringent phase-matching postulated by Armstrong [6] in 1962 for compensating the phase velocity mismatch in various frequency conversion processes. For birefringent materials, even though we have the major problem of walk-off, it is still possible to fulfil both the energy conservation and phase-matching under certain conditions since the refractive index depends on the polarisation of the nonlinear media. In addition to the phase-matching conditions to be satisfied for various frequency conversion processes, efficient nonlinear conversion also requires large

nonlinear optical coefficient (d_{eff}). But there exists many nonlinear materials in which the phase-matching and the energy conservation can be fulfilled simultaneously but the largest nonlinear coefficient could not accessed for frequency conversion processes. As an example, is the well known negative birefringent nonlinear material $LiNbO_3$. Its largest nonlinear coefficient is d_{33}, which implies that the polarisations of the three interacting beams need to be the same. In birefringent phase-matching, this coefficient cannot be accessed either by *type I* or *type II* phase-matching. Thus, an alternate method is necessary to access the largest nonlinear coefficient and this is made possible through the process called quasi-phase-matching.
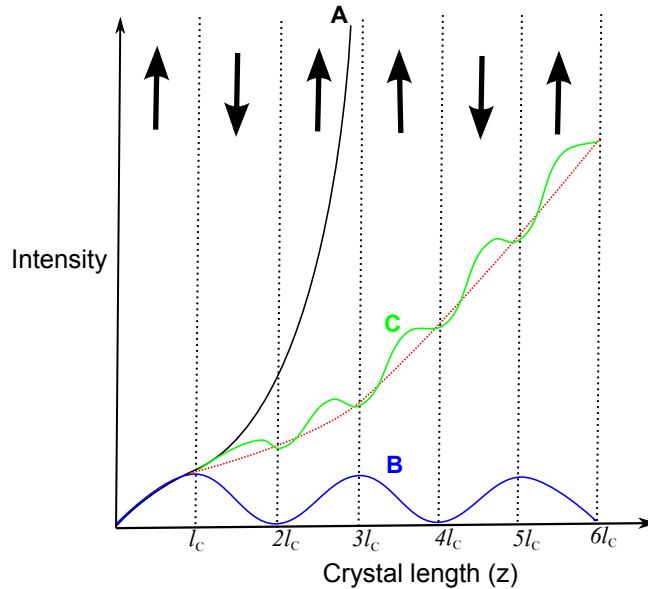
Figure 2.6: Quasi-phase-matching in a periodically poled nonlinear optical material. (A) Perfect phase-matching, (B) Non-phase-matched, and (C) Quasi-phase-matching.

In QPM, the nonlinear coefficient is modulated using a technique called periodical poling, as shown in *Fig*. 2.6. Using this technique, the nonlinear coefficient is modulated with a period twice the coherence length given by $l_c = \frac{\pi}{\Delta k}$. In other words, the nonlinear coefficient changes its sign after each coherence length. Thus, the polarisation is shifted by $180°$ after each coherence length, making the interacting waves propagate in phase along the

crystal length. The relative phase is adjusted by modulating the sign of the nonlinear coefficient of the medium with a period given by $\Lambda = 2l_c$.

From *Fig.* 2.6, although the efficiency in a QPM process is lower than the perfect phase-matching in birefringent materials, QPM is not restricted to *type I* or *type II* phase-matching. Especially with the type 0 (e→ee) process, the largest nonlinear coefficient (d_{33}) for many nonlinear materials can be accessed, which inturn enhances the conversion efficiency to a greater extent. The nonlinear coefficient in the QPM process is given by the relation:

$$d = \frac{2d_{eff}\sin(Dm\pi)}{m\pi} \tag{2.24}$$

where m is the order of QPM and D is the duty cycle ($D = l/\Lambda$).

Another advantage is that QPM usually operates in non-critical phase-matching and hence walk-off angle is zero (as all the involved polarisations are parallel to each other).
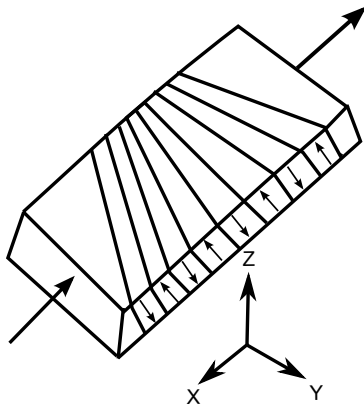
Figure 2.7: Fan-out grating design.

With the development of crystal growth technology of periodic poling since 1990's, periodically poled lithium niobate (popularly known as PPLN) has become most commonly used nonlinear material for various frequency conversion process throughout its transparency range from 400 *nm* in the *visible* region to 5400 *nm* in the *mid-infrared* region. Nowadays fan-out grating poling in the PPLN is used for many OPO applications ever since the design was first used by P. E. Powers [43] in 1998.

The design of the fan-out grating is shown in $Fig.$ 2.7. Fabrication of quasi-phase-matched crystals is done by periodic reversal of the domains in ferro-electric materials such as $LiNbO_3$ and $LiTaO_3$. By applying a strong periodic electric fields ($\sim$21 kV/mm), the spontaneous electronic polarisation of these materials are inverted at room temperature.

2.5 Ultrafast synchronously-pumped optical parametric oscillators

An OPO essentially consists of a nonlinear medium deployed within an optical cavity pumped by a suitable laser source. In analogy, an OPO can be treated as a tunable coherent source but is not a laser by itself. Because in a laser, transitions are governed by the population inversion through energy storage and the tuning depends on bandwidth of the electronic or atomic transitions. On the other hand, in OPOs, there is no storage of energy and the gain is instantaneous. Also, the wavelength tunability is attained by the phase-matching condition in conjunction with the energy conservation laws. Due to this instantaneous nature of the parametric gain, operation of ultrafast pulse OPOs is attainable only under synchronous pumping conditions. The temporal window of the pump pulses is very narrow to allow a sufficient number of round-trips for the build up of the parametric waves over the pump pulse envelope, even for OPO cavity lengths as short as a few millimetres. To circumvent this difficulty, the OPO cavity length is matched exactly to the repetition rate of the pump laser, and hence is known as synchronously-pumped OPO (SPOPO). Thus, the round-trip transit time in the OPO cavity is equal to the repetition period of the pump pulse train. In this way, the resonated parametric waves experience amplification after each round trip through the nonlinear crystal. In practice, the most widely used solid-state KLM Ti:sapphire fs laser has a repetition rate (RR) typically between 76 to 100 MHz. This corresponds to a SPOPO standing wave cavity length ($L = c/2RR$) of 197.4 cm to 150 cm, respectively.

35

SPOPOs offer a number of advantages over the conventional mode-locked lasers. In addition to the broad wavelength tuning, the output pulses from SPOPOs exhibit lower timing jitter relative to the pump pulses. This makes SPOPOs highly suitable for many applications like time resolved spectroscopy, confocal microscopy, pump-probe spectroscopy, etc. The first report of a *fs* SPOPO was made by Edelstein [12] in 1989, based on KTP as the nonlinear medium pumped by a colliding pulse-mode-locked dye laser. However, progress in *fs* SPOPO technology has experienced an unprecedented upsurge with the invention of the Kerr-lens-mode-locked (KLM) Ti:sapphire laser. In today's technology, ultrafast *fs* SPOPOs pumped by solid-state Ti:sapphire laser represent the most advanced class of reliable and robust tunable coherent sources. In this thesis, the main focus or theme is projected in the direction of all solid-state Ti:sapphire-pumped SPOPOs and their potential impact for accessing various spectral regions from *near to mid-infrared*. The configuration of a commercially available solid-state KLM Ti:sapphire laser used for pumping various SPOPOs is shown in the *Fig.* 2.8.

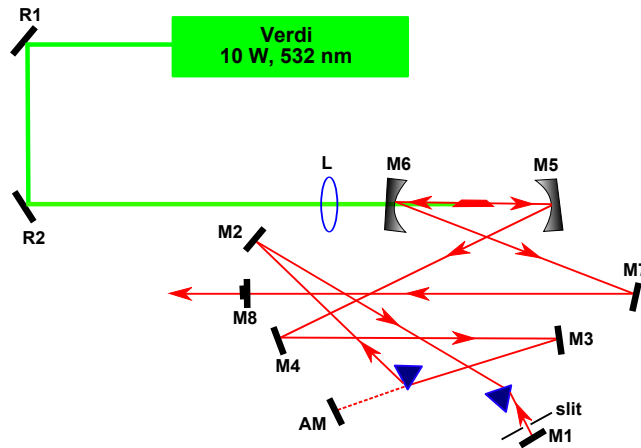Figure 2.8: Schematic of a commercially available solid-state KLM Ti:sapphire laser system used to pump the SPOPOs.

The KLM Ti:sapphire has a repetition frequency of 76 *MHz* and is tunable from $700 - 980$ *nm*. At a central wavelength of 800 *nm*, it delivers an average power of 1.2 W with a spectral bandwidth of 7 *nm* and has a measured interferometric autocorrelation time duration of ∼150 *fs*. Also the schematic

of the Ti:sapphire pumped SPOPO is shown in the *Fig.* 2.9 in a simple standing-wave V-cavity design.
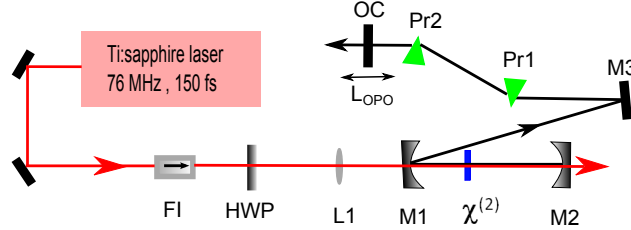
Figure 2.9: Schematic of the SPOPO in standing-wave V-cavity design. The cavity length of the SPOPO is equal to the repetition rate (76 *MHz*) of the pump laser source.

2.6 Gain and amplification in parametric devices

In case of nonlinear optical parametric process, the single-pass amplification in a crystal of length L, is given by

$$G_s(L) = \frac{E_s^2(L)}{E_s^2(o)}) - 1 \simeq \Gamma^2 L^2 \frac{\sinh^2[\Gamma^2 L^2 - (\Delta k L/2)^2]^{1/2}}{[\Gamma^2 L^2 - (\Delta k L/2)^2]} \tag{2.25}$$

where Δk is the phase-mismatch. With I_p as the pump intensity, the gain factor Γ is defined as

$$\Gamma^2 = \frac{8\pi^2 d_{eff}^2}{c\epsilon_o n_s n_i n_p \lambda_s \lambda_i} I_p \tag{2.26}$$

Under perfect phase-matching $\Delta k = 0$, the single-pass amplification in *equation* 2.25 reduces to

$$G_s(L) = \sinh^2(\Gamma L) \tag{2.27}$$

For low gain, $\Gamma L \leq 1$, the *equation* 2.27 can be approximated to

$$G_s(L) = \Gamma^2 L^2 \tag{2.28}$$

and for high gain, $\Gamma L >> 1$, the *equation* 2.27 becomes

$$G_s(L) = \frac{1}{4}e^{2\Gamma L} \tag{2.29}$$

Thus, one can infer that under perfect phase-matching, the single pass amplification is proportional to square of the crystal length (L^2) in case of low gain and increases exponentially in case of high gain.

2.7 Design issues of the OPO

While designing OPOs, the underlying principle is the maximisation of parametric gain through suitable choice of nonlinear medium. Other important parameters are pump laser, favourable phase-matching conditions for obtaining the wavelength tunability, cavity design and optimum focusing. Each of the above mentioned parameters play a crucial role in the process of developing an OPO to make it operate at optimum performance.

2.7.1 Nonlinear material

The selection of the nonlinear material is the heart of the whole OPO system. This selection is governed by many factors such as broad transparency range, phase-matchability in the wavelength of interest, high optical damage threshold, low spatial and temporal walk-off, availability in bulk form, low loss, and if possible, the capability of NCPM. Another important material parameter is the large nonlinear coefficient (d_{eff}), because the parametric gain is directly proportional to the square of the nonlinear coefficient. One often describes the efficiency of the nonlinear medium in terms of *figure of merit (FOM)* defined as

$$FOM \equiv \frac{d_{eff}}{\sqrt{n_p n_s n_i}} \tag{2.30}$$

However, the *FOM* is a convenient parameter to compare nonlinear media for a particular spectral range, but it neglects the effects of absorption and group-velocity mismatch.

2.7.2 Pump laser

The selection of the pump laser plays a major and crucial role in the process of developing any OPO. Because for each nonlinear material, depending upon the phase-matching conditions and for the wavelengths of interest to be generated, it may require a pump source operating at a different wavelength other than the commercially existing lasers. In this case, other alternative methods like cascaded OPOs have to be deployed in which the output of an OPO is used to pump the next consecutive OPO. One obvious criterion is that the pump laser should lie within the transparency range of the nonlinear medium. The pump source must also have sufficient peak intensity (I_p) and low beam divergence to obtain the optimum focussing.

2.7.3 Phase-matchability

The phase-matching behaviour and tuning characteristics of the material can be derived from the conservation of *electromagnetic* momentum or the phase-matching condition $(\Delta k = k_p - k_s - k_i = 0)$ by using the dispersion relations or Sellmeier equations of the nonlinear materials. Also, since the parametric gain has its maximum value at $\Delta k = 0$, the generated wavelengths are determined by the energy conservation, defined as $\omega_p = \omega_s + \omega_i$. And the wavelength tuning is achieved commonly by changing one of the parameter of the nonlinear crystal like angle, temperature, grating, or even by varying the pump wavelength.

2.7.4 Cavity design

Different cavity designs can be configured while deploying the SPOPOs as shown in the *Fig.* 2.8. Extreme care should be taken to determine the stability region of the cavity and for mode-matching the pump beam and the oscillating signal inside the optical resonator. Also due to synchronous pumping, precision within a few micrometers plays a vital role in the process of developing SPOPOs. In general, the optical cavities can be classified into two types.
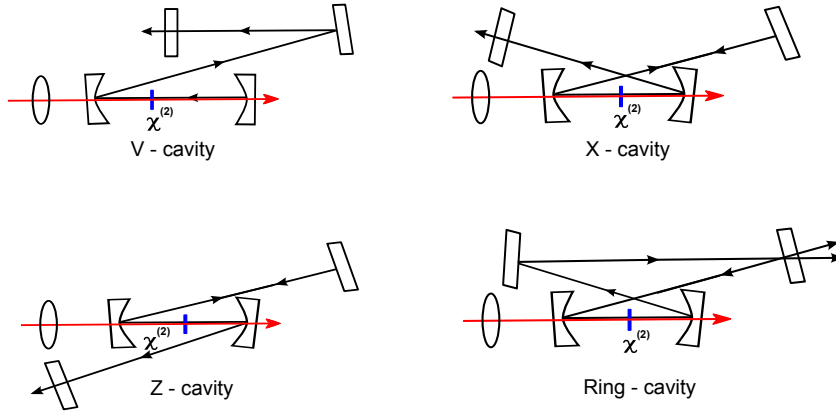
Figure 2.10: Different cavity designs for deploying the SPOPOs. The designs of V, X, Z are known as standing-wave cavities while the ring design is known as travelling-wave cavity.

First one is the standing-wave cavity like V, X, and Z. In these designs, the oscillating fields transits twice through the nonlinear medium in a round trip. The second one is travelling-wave ring cavity in which the oscillating field transits only once through the nonlinear crystal per round trip thus providing extra reduction in the losses due to absorption and crystal coatings. One particular advantage of using ring cavity design is that it avoids the optical feedback into the laser system.

Also for attaining optimum performance of an OPO, the confocal parameter of the pump beam, b_p, which is twice the Rayleigh range, needs to be equal to that of the resonating beam b_s ($\sim b_p$). For more information on stability criteria, ABCD and transformation matrices, one can refer to *Laser electronics* [44] by Verdeyen and *the classic paper* of Kogelnik and Li [45].

2.8 Dispersion characteristics

Dispersion characteristics like group velocity, group velocity mismatch (GVM) and group velocity dispersion (GVD) play very important role in the ultrafast *fs* regime [46], [47].

2.8.1 Group velocity

An ultrafast pulse can be imagined as quasi-monochromatic, and hence is composed of several frequencies clustered about some central frequency ω_o that can be considered as the *carrier frequency* of the wave. Under the condition where dispersion in the refractive index cannot be ignored with the pulse propagation inside the medium, the concept of unique phase velocity becomes meaningless, and the pulse itself should be treated as superposition of monochromatic waves lying under a *carrier wave envelope.* This is characterised by the group velocity defined as

$$v_g = \frac{d\omega}{dk}\big|_{\omega_o} \tag{2.31}$$

The group velocity of a pulse propagating in a medium is defined as

$$v_g = \frac{c}{n - \lambda\dfrac{dn}{d\lambda}} \tag{2.32}$$

where c is the velocity of light in vacuum, n is the refractive index of the nonlinear medium, and λ is the central wavelength.

2.8.2 Group velocity mismatch (GVM)

In various nonlinear frequency mixing processes and devices such as SHG, SFG, DFG, OPO and OPA, two or more waves interact with each other while propagating through the nonlinear medium. Due to the dispersion of the nonlinear medium, different waves propagate at different group velocities and thus the interacting pulses will get completely separated after a certain distance in the medium. This physical temporal separation between the pulses thus causes a reduction in effective interaction length between the interacting waves. In *fs* regime, while propagating through a nonlinear medium, the quantitative evaluation of this temporal pulse separation with distance is characterised by group velocity mismatch (GVM). The GVM is

defined as

$$GVM = |(\frac{1}{v_{g,i}} - \frac{1}{v_{g,j}})|^{-1} \tag{2.33}$$

where $v_{g,i}$ and $v_{g,j}$ are the group velocities of the interacting waves i and j, respectively.

The GVM dictates the phase-matching bandwidth and the maximum effective interaction length that can be used for any frequency conversion process. As an example, we derive here the dependence of phase-matching bandwidth on the GVM in a SHG process [48].

2.8.3   Phase-matching bandwidth

Consider that the pulse at fundamental wavelength λ_o is propagating through a nonlinear crystal and the generated SHG is at wavelength $\lambda_o/2$. Since both the fundamental and SHG waves have different group velocities, there will be a mismatch between these two interacting waves. The two pulses cease to overlap after propagating some distance L inside the crystal. We can calculate the bandwidth of the SHG pulses when GVM is taken into consideration. Assuming that a very short pulse enters the crystal, the time lapse for the SHG pulse, δt, can be determined by the difference between the time durations of the fundamental and SHG waves given by:

$$\delta t = \frac{L}{v_g(\lambda_o/2)} - \frac{L}{v_g(\lambda_o)} = L\,GVM \tag{2.34}$$

where GVM $= \dfrac{1}{v_g(\lambda/2)} - \dfrac{1}{v_g(\lambda)}$. Rewriting this equation in terms of group velocity defined as

$$v_g(\lambda) = \frac{c/n(\lambda)}{1 - (\lambda/n(\lambda))n'(\lambda)} \tag{2.35}$$

and substituting for the group velocities in equation 2.34, we get

$$\delta t = L\frac{n(\lambda_o/2)}{c}[1 - \frac{\lambda_o/2n'(\lambda_o/2)}{n(\lambda_o/2)}] - L\frac{n(\lambda_o)}{c}[1 - \frac{\lambda_o n'(\lambda_o)}{n(\lambda_o)}] \tag{2.36}$$

Now considering the fact that under perfect phase-matching, $n(\lambda/2) = n(\lambda)$, the above equation can be rewritten as

$$\delta t = \frac{L\lambda_o}{c}[n'(\lambda_o) - \frac{1}{2}n'(\lambda_o/2)] \tag{2.37}$$

Assuming that the second-harmonic pulse has a Gaussian intensity, for which $\delta t \delta\nu = 0.44$, in terms of wavelength it becomes

$$\delta t \delta\lambda = \delta t \delta\nu [\frac{d\nu}{d\lambda}]^{-1} = -0.44\frac{\lambda^2}{c} \tag{2.38}$$

The minus sign can be neglected since we are computing the bandwidth, which is inherently positive. So the phase-matching bandwidth can be written in terms of wavelength as follows:

$$\delta\lambda = \frac{0.44\lambda_o/L}{[n'(\lambda_o) - \frac{1}{2}n'(\lambda_o/2)]} \tag{2.39}$$

Therefore, from the above equation, we can infer the following:
The phase-matching bandwidth $\delta\lambda$, is inversely proportional to the length of the nonlinear crystal.
Since an ultrashort pulse can have extremely broad bandwidth (as an example a 10 *fs* pulse centred at 800 *nm* will have a bandwidth of $\sim$100 *nm*), to achieve efficient phase-matching for the entire bandwidth of the pulse, it is necessary to use extremely thin (as thin as 5 *μm*) SHG crystals.
Also, recalling from *equation* 2.28 the parametric gain of the phase-matched process is directly proportional to L^2, so a very thin crystal yields a lower output intensity or conversion efficiency.
Thus in the ultrafast fs *regime, there always exists a trade-off between efficiency and bandwidth.*
The phase-matching bandwidth can also be computed in frequency domain by expanding phase-mismatch (Δk) as a function of wavelength in Taylor's series expansion [48].

2.8.4 Effective interaction length

As mentioned before, the crystal length is limited by the GVM between the interacting waves. In case of OPO, we mainly take into account the GVM between the pump and the oscillating signal pulses. Assuming that the signal and pump have the similar pulse duration, τ_p, the effective crystal length can be computed by using the following formula:

$$L_{eff} \leq 2\,\tau_p \mid \Delta v_g \mid \leq 2\tau_p|\frac{1}{v_{g,p}} - \frac{1}{v_{g,s}}|^{-1} \tag{2.40}$$

where L_{eff} is the effective interaction length and $v_{g,p}$, $v_{g,s}$ are the group velocities of pump and signal pulses, respectively. The practical crystal length is normally longer than L_{eff}. In case of sub-100 *fs* pulses, the crystal length should be chosen as thin as $L_{eff}/4$ [49].

Thus in any nonlinear frequency conversion process, GVM between the interacting waves is an important factor leading to pulse broadening in ultrafast fs *regime. Together with the pump pulse duration and the expected signal pulse duration, it determines the effective interaction length.*

2.8.5 Spectral acceptance bandwidth

The spectral acceptance bandwidth (SAB) is another important parameter to be considered in ultrafast *fs* regime. The large spectral bandwidth of *fs* pulses imposes severe restrictions on the maximum usable crystal length. Also, it sets an upper limit to the maximum allowable pump bandwidth before the parametric gain severely diminishes. In general SAB depends on the type of phase-matching and the dispersion properties of the nonlinear medium. For an OPO, the SAB can be computed using the GVM between the interacting waves given by

$$\Delta \lambda L = \frac{\lambda^2}{2\pi c} \frac{2.78}{(GVM)_{i,j}} \tag{2.41}$$

SAB has the units of *nm.cm*. *Thus, the SAB provides the information about the maximum usable length of the nonlinear medium and the maximum allowed pump spectral bandwidth for attaining optimum parametric gain in a frequency conversion process.*

2.8.6 Group velocity dispersion (GVD)

When dispersion cannot be ignored, the propagating pulse will no longer have the simple form and the dispersion will cause the pulse amplitude to decrease and spread out as the pulse propagates. Then the group velocity itself will exhibit dispersion, which is characterised by the group velocity dispersion coefficient defined by

$$k'' = \frac{d(v_g)^{-1}}{d\omega} = \frac{d^2k}{d\omega^2} \tag{2.42}$$

In terms of wavelength, it can be written as :

$$k'' = \frac{\lambda^3 L}{2\pi c^2} \frac{d^2n}{d\lambda^2} \tag{2.43}$$

In ultrafast *fs* regime, GVD is an important parameter to evaluate the dispersion characteristics of gain media or in this case the nonlinear medium to be deployed inside the optical resonator. Based on GVD, we can estimate the degree of pulse broadening, and thus can design a proper dispersion compensation mechanism. Also, the pulse broadening induced by the GVD, when the pulses propagate through a nonlinear material of length (z), is given by

$$\tau_p(z) = \tau_o \sqrt{1 + (\frac{z}{z_d})^2} \tag{2.44}$$

where τ_o is the original pulse duration before entering the dispersive medium, τ_p is the pulse duration after passing through the dispersive material, and z_d is the characteristic length defined as

$$z_d = \frac{1}{4ln2} \frac{\tau_0^2}{\frac{d^2k}{d\omega^2}} \tag{2.45}$$

Thus, control of dispersion is an important key to obtain short and transform-limited pulses.

Two commonly used methods for manipulating the GVD are prism sequence and grating pairs. Both of these methods involve optical components with angular dispersion. Alternative methods include chirped mirrors [50] or wedges made up of materials which inherently possesses the negative GVD, can also be used for GVD compensation. Here we describe the dispersion compensation using a prism pair [51], [46] which is the most common method used in ultrafast optics. Compared to gratings, the main advantage of using prisms is the low loss, which makes them suitable for dispersion compensation control inside the optical resonators, as well as easy tuning of the sign and magnitude of the dispersion.

2.8.7   GVD compensation using a prism pair

The configuration consists of a pair of anti-parallel prisms. The various frequencies in the collimated input beam emerge from the first prism with different angles, but travel in parallel directions after the second prism. While the angular dispersion between the prisms contributes anomalous or negative GVD, the passage through the prism material is also a source of normal dispersion. The overall dispersion can be tuned by translating one of the prisms in a direction perpendicular to its base, which varies the material path length without affecting the angular dispersion.

As shown in the *Fig.* 2.9, the first prism is oriented at Brewster angle for the beam to incident at its apex (P_o). The dispersed beam after the first prism is made to be incident at the apex of the second prism (Q_o), which is also oriented at Brewster angle.

Both the prisms are arranged in such a manner that their apexes are aligned in opposite direction. The angular dispersion occurring between the two prisms is designated by the angle $\alpha(\lambda)$, which is a function of wavelength. Since $\alpha(\lambda)$ is very small, the wavefront at $\overline{P_1 P_2}$ has approximately the same phase at $\overline{P'_1 P'_2}$. The optical path length of $\overline{P_0 P_1}$ corresponds to the shortest spectral component of the incident beam. At point P_1, the optical path

length of any other spectral components can be expressed as

$$l(\lambda) = \overline{P_0P_1}cos\alpha, \tag{2.46}$$

and the phase delay can be written as :

$$\psi_\alpha = \frac{2\pi}{\lambda}\overline{P_0P_1}cos\alpha \tag{2.47}$$
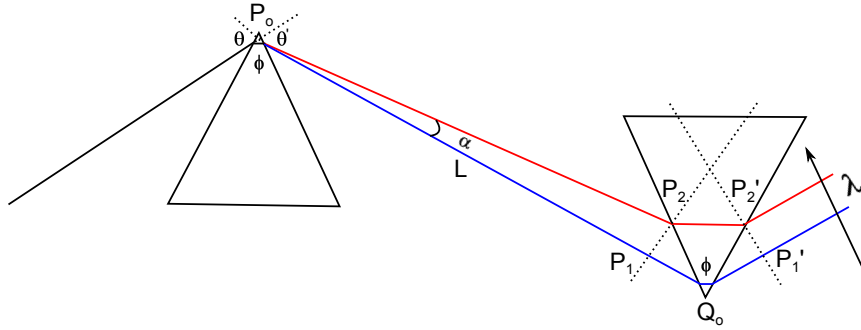

Figure 2.11: Schematic of the prism pair for GVD compensation in ultrafast *fs* regime.

As α is very small and the distances between the two prisms, $\overline{P_0P_1}>>\overline{P_1Q}$, $\overline{P_0P_1}$ can be approximated to the distance between the prisms (L), and the above equation can be rewritten as

$$\psi_\alpha = \frac{2\pi}{\lambda}Lcos\alpha = \frac{\omega}{c}Lcos\alpha. \tag{2.48}$$

Then, the GVD induced by the angular dispersion by prisms can be derived from following *equation.*

$$\frac{d^2\psi_\alpha}{d\omega^2} = -\frac{L}{c}\{\sin\alpha[2\frac{d\alpha}{d\omega} + \omega\frac{d^2\alpha}{d\omega^2}] + \omega\cos\alpha(\frac{d\alpha}{d\omega})^2\} \tag{2.49}$$

Since α is very small, we can assume that $\sin\alpha \sim 0$ and $\cos\alpha \sim 1$.

Then the GVD can be rewritten as

$$\frac{d^2\psi_\alpha}{d\omega^2} = -\frac{\omega L}{c}(\frac{d\alpha}{d\omega})^2 \tag{2.50}$$

From the above equation, we can infer that the GVD induced by the prism pair is negative, and thus can be used to compensate the positive GVD induced by the nonlinear gain medium.

To compute the value of $(\frac{d\alpha}{d\omega})$, consider

$$\frac{d\alpha}{d\omega} = \frac{d\alpha}{dn}\frac{dn}{d\alpha} \quad and \quad \frac{dn}{d\alpha} = -\frac{\lambda^2}{2\pi c}\frac{dn}{d\lambda} \tag{2.51}$$

where n is the refractive index of the prism material. To calculate $\frac{d\alpha}{dn}$, consider the geometry of the prism as shown in $Fig.$ 2.10.
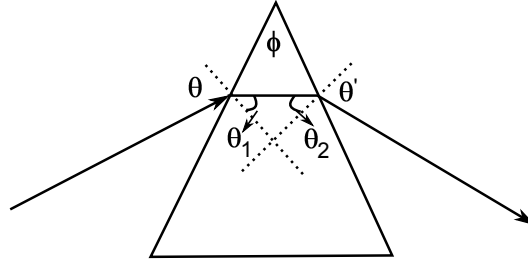

Figure 2.12: Geometry of a single prism showing the apex angle, angle of incidence and refracted rays.

The following relationships can be written from the geometry of the prism

$$\sin\theta = n\sin\theta_1 \tag{2.52}$$

$$\sin\theta' = n\sin\theta_2 \tag{2.53}$$

$$\theta1 + \theta2 = \phi \tag{2.54}$$

From the above equations we can obtain

$$\cos\theta\frac{d\theta}{dn} = \sin\theta_1 + n\cos\theta_1\frac{d\theta_1}{dn} \tag{2.55}$$

48

$$\cos\theta'\frac{d\theta'}{dn} = \sin\theta_2 + n\cos\theta_2\frac{d\theta_2}{dn} \tag{2.56}$$

$$\frac{d\theta_1}{dn} = -\frac{d\theta_2}{dn} \tag{2.57}$$

Since θ is fixed, $\dfrac{d\theta}{dn} = 0$, we can derive that

$$\frac{d\theta_1}{dn} = -\frac{d\theta_2}{dn} = \frac{1}{n}\tan\theta_1 \tag{2.58}$$

and we can compute

$$\frac{d\theta'}{dn} = \frac{\sin\theta_2}{\cos\theta'} + \frac{\cos\theta_2}{\cos\theta'}\tan\theta_1 \tag{2.59}$$

Considering the Brewster angle of incidence at λ_o, $\theta' = \theta$ and $\theta_1 = \theta_2$, and substituting in equation 2.59, we get

$$\frac{d\theta'}{dn}\mid_{\lambda_o} = 2 \tag{2.60}$$

From $Figs.$ 2.9 and 2.10, we can conclude that, $\dfrac{d\alpha}{dn} = \dfrac{d\theta'}{dn}$, and substituting in equation 2.50 for GVD, we get

$$\frac{d^2\psi_\alpha}{d\omega^2}\mid_{\lambda_o} = -4L\frac{\lambda^3}{2\pi c^2}\left(\frac{dn}{d\lambda}\right)^2 \tag{2.61}$$

This is the final expression for the single-path negative GVD created by the prism pair.

As the beam propagate through some amount of the prism material, an additional GVD will be induced by the prisms, which should also be taken into account while calculating the total amount of GVD created by the prism pair. Assuming l to be mean amount of glass material path through the prisms, the positive GVD introduced by prism pair can be written as

$$\frac{d^2\psi_p}{d\omega^2}\mid_{\lambda_o} = \frac{\lambda^3 l}{2\pi c^2}\frac{d^2 n}{d\lambda^2} \tag{2.62}$$

If we know the material of prisms, $\dfrac{d^2 n}{d\lambda^2}$ can be determined. Therefore, we need to find the mean path length (l) of glass that the pulses propagate through. If the beam diameter is D, ϕ is the apex angle of the prisms, θ is the Brewster angle for the prism material and $\Delta\lambda$ is the spectral bandwidth of the incident pulses, the mean path length l is given by

$$l = \frac{2[D + \Delta\lambda L \dfrac{dn}{d\lambda}]\sin\dfrac{\phi}{2}}{\cos\theta} \tag{2.63}$$

Thus, the equation for the positive GVD induced by the prism pair can be written as

$$\frac{d^2\psi_p}{d\omega^2}\mid_{\lambda_o} = \frac{\lambda^3 l}{2\pi c^2}\frac{2[D + \Delta\lambda L\dfrac{dn}{d\lambda}]\sin\dfrac{\phi}{2}}{\cos\theta}\frac{d^2 n}{d\lambda^2} \tag{2.64}$$

Therefore, the final expression for the total GVD can be written as

$$\frac{d^2\psi_T}{d\omega^2}\mid_{\lambda_o} = \frac{d^2\psi_\alpha}{d\omega^2}\mid_{\lambda_o} + \frac{d^2\psi_p}{d\omega^2}\mid_{\lambda_o} \tag{2.65}$$

Thus, the overall dispersion can be tuned by translating one of the prisms in a direction perpendicular to its base, which varies the material path length without affecting the angular dispersion.

2.9 SPOPO tuning methods

As mentioned before, the main strength of an OPO is its tunability. Traditionally known wavelength tuning methods are carried out by changing one of the parameter of the nonlinear medium like:

1. Angle
2. Temperature
3. Grating

Pump tuning can also be achieved by tuning the wavelength of pump laser source. *Besides the above traditional methods, in the ultrafast* fs *regime, the wavelength tunability can also be achieved by varying the cavity length of the SPOPO.*

2.9.1 Cavity length tuning

The cavity length tuning is mainly governed by the dispersion characteristics of the nonlinear material. The cavity length tuning can be understood as follows:

For the case of positive GVD, when the cavity length is increased, the signal wavelength has to shift to a longer wavelength side to maintain the synchronization with the pump pulse. Similarly, a shorter signal wavelength oscillates at a shorter cavity length.

For the case of negative GVD, the opposite process will take place. [33]